

## Time delay, resonances, Riemann zeros and chaos in a model quantum scattering system

This article has been downloaded from IOPscience. Please scroll down to see the full text article.

1989 J. Phys. A: Math. Gen. 22 3561

(<http://iopscience.iop.org/0305-4470/22/17/021>)

View [the table of contents for this issue](#), or go to the [journal homepage](#) for more

Download details:

IP Address: 129.252.86.83

The article was downloaded on 31/05/2010 at 11:48

Please note that [terms and conditions apply](#).

## Time delay, resonances, Riemann zeros and chaos in a model quantum scattering system

David M Wardlaw† and Wojciech Jaworski‡

Department of Chemistry, Queen's University, Kingston, Ontario K7L 3N6, Canada

Received 17 May 1988

**Abstract.** The quantum treatment of an intrinsically chaotic model scattering system originally studied by Gutzwiller is extended to include the time delay and to make explicit the zeros of the Riemann zeta function in the mathematical expressions for the scattering matrix  $S$  and the time delay. The system consists of a particle moving on a two-dimensional surface of constant negative curvature. The scattering in this unusual system is dominated by resonances associated with poles of  $S$  in the complex momentum plane; the real parts of these poles are one-half of the imaginary parts of the Riemann zeros. The resonances have a constant width but their average spacing varies with the momentum. The focal point is the manifestation of chaotic behaviour in the time delay. Features considered in this regard include: the momentum dependence of the time delay in regions of overlapping and isolated resonances, the decomposition of the time delay into an average (dynamical) component and a fluctuating (chaotic) component, and characterisation of the fluctuating component by its autocorrelation function.

### 1. Introduction

The motion of a free particle on a surface of constant negative curvature (a pseudosphere) has long been known to provide a well defined and tractable example of a conservative dynamical system displaying chaotic classical motion [1]. A large number of such systems, undergoing either bound or unbound motion, can be defined by specification of suitable boundary conditions (or, equivalently, by suitable tessellations of the surface); general features and categories of these systems have been discussed by Series [1]. Some recent work [2] focused on the quantum dynamics of a particular bound system on the pseudosphere in order to elucidate the meaning of quantum chaos and its relation to the known classical chaos. Here we extend Gutzwiller's quantum mechanical treatment [3] of a particular unbound system on the pseudosphere. One of our motivations for this extension is to cast theoretical and numerical results in forms compatible with traditional scattering theory interpretations of chaotic dynamics. We begin by describing the unusual nature of the scattering system.

It consists of a particle of mass  $m$  moving in the upper half-plane  $\mathcal{L} = \{(x, y) \in \mathbb{R}^2 | y > 0\}$ , with time-independent Hamiltonian

$$H = \frac{-\hbar^2}{2m} y^2 \left( \frac{\partial^2}{\partial x^2} + \frac{\partial^2}{\partial y^2} \right) - \frac{\hbar^2}{8m}. \quad (1.1)$$

† NSERC of Canada University Research Fellow.

‡ On leave from: Institute of Physics, Nicholas Copernicus University, Torun, Poland.

The half-plane  $\mathcal{L}$  is equipped with non-Euclidean metric  $ds^2 = y^{-2}(dx^2 + dy^2)$ , thus becoming a Riemannian space with constant negative curvature. The scattering is non-conventional since it is not the result of interparticle forces but can be imagined to arise from (physically non-realisable) constraint forces, i.e. the curvature of the space. As explained in some detail by Gutzwiller [3], the Hamiltonian  $H$  is the quantum mechanical counterpart of the classical Hamiltonian

$$H_{cl} = \frac{y^2}{2m} [p_x^2 + p_y^2] \quad (1.2)$$

describing free motion in  $\mathcal{L}$ , i.e. motion along geodesics with constant velocity

$$v = \frac{ds}{dt} = \left\{ y^{-2} \left[ \left( \frac{dx}{dt} \right)^2 + \left( \frac{dy}{dt} \right)^2 \right] \right\}^{1/2} = \sqrt{2H_{cl}/m}. \quad (1.3)$$

Construction of the corresponding quantum mechanical scattering solutions for the Schrödinger equation  $i\hbar \partial\psi/\partial t = H\psi$  requires careful specification of boundary conditions in  $\mathcal{L}$ . This procedure is non-trivial and is not discussed here; the interested reader is referred to [3–6].

The asymptotic scattering solutions and associated scattering quantities (phase shift, scattering matrix and time delay) turn out to be conveniently specified in terms of known functions. One of these functions is Riemann's zeta function whose appearance signals some sort of chaos, several features of which have been discussed in [3].

In § 2 we introduce the time delay which, as in conventional elastic scattering, is the energy derivative of the phase shift. The study of this time delay is the central feature of the paper. Gutzwiller has interpreted, at relatively small values of the 'momentum'  $w$ , the qualitative behaviour of the phase shift in terms of the Riemann zeros, i.e. the zeros of the Riemann  $\zeta$  function. In § 3 we make this connection explicit for the scattering matrix and the time delay. In particular, the real parts of the poles of the scattering matrix in the complex momentum plane are one half of the imaginary part of the Riemann zeros and the time delay expression obtained in § 2 is recast in terms of the zeros. Numerical results for the time delay and several of its properties are discussed in § 4.

Our primary motivation for this study is the investigation of time delay in a scattering system which is in some sense chaotic. The convenience of the model lies in the availability of a dynamically exact time delay expression. Ultimately we are interested in the chaotic attributes of collision lifetimes in conventional scattering systems (for which exact time delay expressions are generally unobtainable) and hope that the present study will provide useful background for such studies. We test a general idea recently summarised by Weidenmüller [7] concerning the nature of chaos in quantum systems and which here amounts to considering that the momentum dependence of the time delay might be usefully expressed as average behaviour on which is superimposed a fluctuating component containing generic or universal behaviour. Another interesting feature is that the scattering, and hence the time delay, is strongly influenced by resonances whose widths are constant and whose positions are determined by the Riemann zeros, the latter having a nearest-neighbour spacing distribution and pair correlation function which are well described by the Gaussian unitary ensemble (GUE) [8]. As  $w$  increases, the average spacing between neighbouring resonance levels decreases, eventually resulting in overlapping resonances when the mean spacing is less than the width. The appearance of the Riemann zeros in the model system is of interest in its own right. It has been proposed [9, 10] to treat the imaginary parts of

the zeros as eigenvalues of some unknown Hermitian operator and there is speculation [11] that the statistical properties of these (bound state) eigenvalues may provide a useful model of quantum chaos. Here the zeros arise without assumption or approximation in a well defined, albeit unusual, system and instead of describing bound states, they determine quasibound resonance scattering states.

## 2. Scattering quantities

### 2.1. Asymptotic scattering solutions

Asymptotic ( $y \rightarrow \infty$ ) solutions of the time-independent Schrödinger equation are known [1, 3-6] to depend only on  $y$  and to have the following form†:

$$\psi_w(x, y) \approx y^{1/2} [y^{-iw} + S(w)y^{iw}] \quad \text{as } y \rightarrow \infty \quad (2.1)$$

where  $w = (2E)^{1/2}$  is the ‘momentum’ associated with energy  $E$  (both  $m$  and  $\hbar$  are set to unity for the remainder of the paper). The quantity  $S(w)$  in (2.1) is the scattering matrix [4, 5]. It is complex and is determined by the gamma ( $\Gamma$ ) function and Riemann’s zeta ( $\zeta$ ) function:

$$S(w) = \frac{\pi^{-iw} \Gamma(\frac{1}{2} + iw) \zeta(1 + 2iw)}{\pi^{iw} \Gamma(\frac{1}{2} - iw) \zeta(1 - 2iw)}. \quad (2.2)$$

Since  $\Gamma(\frac{1}{2} + iw) = \Gamma(\frac{1}{2} - iw)^* \neq 0$  and  $\zeta(1 + 2iw) = \zeta(1 - 2iw)^* \neq 0$  for  $w \in \mathbb{R}$ ,  $S(w)$  is unimodular and can be written

$$S(w) = \exp[i\delta(w)] \quad (2.3)$$

where  $\delta(w) \in \mathbb{R}$ .

The time dependence of the asymptotic solutions is trivially obtained from the time-dependent Schrödinger equation, yielding

$$\begin{aligned} \psi_{w,t}(x, y) &= e^{-iE(w)t} \psi_w \\ &\approx y^{1/2} [\exp\{-i[E(w)t + w \ln y]\} \\ &\quad + \exp\{-i[E(w)t - w \ln y - \delta(w)]\}] \quad \text{as } y \rightarrow \infty. \end{aligned} \quad (2.4)$$

Upon substitution of  $\theta = \ln y$  this becomes a superposition of plane waves multiplied by the factor  $\sqrt{y} = e^{\theta/2}$  (which is in fact connected with the definition of the scalar product in the Hilbert space of our system [4, 5]). One of the plane waves moves ‘inwards’ with phase velocity  $v_- = -E(w)/w = -w/2$  and the other ‘outwards’ with phase velocity  $v_+ = w/2$ . Following Gutzwiller’s interpretation, the second wave results from scattering (reflection) of the first wave and, accordingly,  $\delta(w)$  is designated as the phase shift. Several relevant features of the phase shift are identified in § 2.2.

Besides scattering of ‘plane waves’ one can also consider scattering of wavepackets. This leads to the concept of time delay, which turns out to be the energy derivative of the phase shift, exactly as in conventional elastic scattering theory. To see this let us introduce wavepackets  $\chi_t(x, y)$  formed from a continuous superposition of the

† Gutzwiller arbitrarily introduces the factor  $\alpha^{iw}$  ( $\alpha > 0$ ) in his incident wave [3] and thereby defines the place for zero phase of the *incident wave* to be  $y = \alpha$ . This factor then leads to a trivial modification of the phase shift and the time delay, leaving the fluctuating parts of these quantities unaltered. Therefore, we decided to drop the factor (put  $\alpha = 1$ ) at the very beginning.

eigenfunctions  $\psi_{wt}(x, y)$  multiplied by a suitable amplitude function  $A(w)$ . When  $A(w)$  vanishes outside a very narrow interval  $[w, w + \Delta]$  such a wavepacket is subject to the standard approximate analysis [12] involving the concepts of group velocity and time delay. For  $t \rightarrow -\infty$  we have the ingoing packet:

$$\chi_t^{\text{in}}(x, y) \approx y^{1/2} \exp\{-i[E(w)t + w \ln y]\} \int_0^\Delta d\eta A(w + \eta) \times \exp\left[-i\eta\left(\ln y + \frac{dE(w)}{dw} t\right)\right] \quad (2.5)$$

which moves with group velocity  $v_g = dE(w)/dw = w$ . For  $t \rightarrow +\infty$  we have the phase-shifted outgoing packet

$$\chi_t^{\text{out}}(x, y) \approx y^{1/2} \exp\{-i[E(w)t - w \ln y - \delta(w)]\} \int_0^\Delta d\eta A(w + \eta) \times \exp\left[-i\eta\left(-\ln y + \frac{dE(w)}{dw}(t - T(w))\right)\right] \quad (2.6)$$

which also moves with group velocity  $v_g$  but is delayed or advanced in time by the so-called time delay

$$T(w) = w^{-1} d\delta(w)/dw \quad \text{or} \quad T(\sqrt{2E}) = d\delta(\sqrt{2E})/dE. \quad (2.7)$$

Strictly speaking, a rigorous justification of  $\delta$  and  $T$  as the phase shift and time delay requires that these quantities be properly defined with respect to some reference system. In conventional scattering systems (i.e. collisions in Euclidean space mediated by an interaction potential) a reference system is established by switching off the interaction potential, in which case the reference phase is zero and the reference time is a (energy-dependent) free particle transit time. Here there is no interaction potential but a reference system can nevertheless be established [4]. For the general case in which the wavepacket is not narrow enough to justify (2.5)–(2.7) a rigorous theoretical definition of the time delay awaits further mathematical development [13]. It is conceivable that assessment of the time delay in the general case may require following the time evolution of scattered and unscattered packets numerically; such calculations, although feasible, are computationally intensive. Here we present time delay results only for arbitrarily narrow wavepackets (i.e.  $T(w)$  in (2.7)); further studies on broader wavepackets are in progress.

## 2.2. The phase shift

Equation (2.3) yields

$$\begin{aligned} \delta(w) &= \text{Arg } S(w) \\ &= -2w \ln \pi + 2 \text{Arg } \Gamma(\tfrac{1}{2} + iw) + 2 \text{Arg } \zeta(1 + 2iw) \\ &= \delta_{\text{bg}} + \delta_{\text{n}} \end{aligned} \quad (2.8)$$

with the functions  $\text{Arg } \Gamma(\tfrac{1}{2} + iw)$  and  $\text{Arg } \zeta(1 + 2iw)$  uniquely defined by the requirements

$$\begin{aligned} \lim_{w \rightarrow +0} \text{Arg } \Gamma(\tfrac{1}{2} + iw) &= 0 \\ \lim_{w \rightarrow +0} \text{Arg } \zeta(1 + 2iw) &= -\pi/2. \end{aligned} \quad (2.9)$$

The identification of a ‘background’ component

$$\delta_{bg}(w) = -2w \ln \pi + 2 \operatorname{Arg} \Gamma(\frac{1}{2} + iw) \tag{2.10}$$

of the phase shift is motivated by its relatively slow variation with  $w$ :  $\delta_{bg}$  increases monotonically from 0 at  $w = 0$  and has simple asymptotics for  $w \rightarrow \infty$ , resulting from the usual Stirling formula [14]:

$$\delta_{bg}(w) \approx 2w[\ln(w/\pi) - 1] \quad \text{as } w \rightarrow \infty. \tag{2.11}$$

The interesting part of the phase shift is its ‘fluctuating’ component

$$\delta_n(w) = 2 \operatorname{Arg} \zeta(1 + 2iw). \tag{2.12}$$

Such a description is motivated by the rapid variation of this quantity, relative to  $\delta_{bg}$ , as is immediately evident in plots (not shown here) of  $\delta_{bg}$  and  $\delta_n$  against  $w$ . The reader is referred to figures 5–7 of [3] for plots of  $\delta_n/2$  on three widely separated  $w$  ranges. At  $w = 0$ ,  $\delta_n$  has the value  $-\pi$ ; as  $w$  increases  $\delta_n$  fluctuates in an increasingly complicated manner. The following bound can, however, be established [15]:

$$\delta_n(w) = O(\ln 2w) \quad \text{as } w \rightarrow \infty. \tag{2.13}$$

Gutzwiller [3] has discussed two interesting features of the  $\zeta$  function: its ability to mimic other functions and its difficulty of evaluation, both of which suggest the stochastic or chaotic character of the model scattering system. He also points out, based on graphical analysis at relatively small  $w$  values, that the detailed structure of  $\delta_n$  as a function of  $w$  is closely related to the zeros of the  $\zeta$  function. In § 3 we make the relationship between the Riemann zeros and the scattering matrix and time delay explicit for all  $w$  values.

### 2.3. The time delay

Differentiating the phase shift (2.8) with respect to energy yields the time delay

$$\begin{aligned} T &= d\delta(\sqrt{2E})/dE \\ &= w^{-1} d\delta(w)/dw \\ &= w^{-1} \left[ -2 \ln \pi + 2 \operatorname{Re} \left( \frac{\Gamma'(\frac{1}{2} + iw)}{\Gamma(\frac{1}{2} + iw)} \right) + 4 \operatorname{Re} \left( \frac{\zeta'(1 + 2iw)}{\zeta(1 + 2iw)} \right) \right] \\ &= w^{-1}(\tau_{bg} + \tau_n) \end{aligned} \tag{2.15}$$

where  $\tau_{bg}$  and  $\tau_n$  are the  $w$  derivatives of  $\delta_{bg}$  and  $\delta_n$ , respectively,  $T_{bg} = \tau_{bg}/w$ , and  $T_n = \tau_n/w$ . The background component  $\tau_{bg}$  is a slowly varying function of  $w$ , increasing monotonically from  $-2 \ln \pi - 2\gamma - 4 \ln 2$  ( $\gamma = 0.577 21 \dots$  is Euler’s constant) at  $w = 0$  and having asymptotics [14]:

$$\tau_{bg}(w) \approx 2 \ln(w/\pi) \quad \text{as } w \rightarrow \infty. \tag{2.16}$$

At  $w = 0$ , the fluctuating component  $\tau_n$  has the value  $4\gamma$  and at large  $w$  its asymptotic bound is analogous to that of  $\delta_n$  [15]:

$$\tau_n(w) = O(\ln 2w) \quad \text{as } w \rightarrow \infty. \tag{2.17}$$

That  $\tau_n$  is rapidly varying relative to  $\tau_{bg}$  is easily seen in one of the figures to be discussed in § 4. Note that the time delay is related to the scattering matrix by  $-iS^*(E) dS(E)/dE = T(\sqrt{2E})$  which has the same form as Smith’s result [16] for elastic scattering.

### 3. Appearance of the Riemann zeros

For the purposes of interpretation and subsequent computation it is useful to express both the scattering matrix  $S$  and the time delay  $\tau$  in terms of the non-trivial zeros of  $\zeta(s)$ , the so-called Riemann zeros.

#### 3.1. Resonances and poles of the scattering matrix

Standard analytic continuation of  $S$  (2.2) into the complex momentum plane [12] yields

$$S(z) = \pi^{-2iz} \frac{\Gamma(\frac{1}{2} + iz)\zeta(1 + 2iz)}{\Gamma(\frac{1}{2} - iz)\zeta(1 - 2iz)} \quad (3.1)$$

where  $z = w + i\alpha$ . The poles  $\xi$  of  $S(z)$  are determined by the zeros of  $\zeta(s)$ , where  $s = 1 - 2iz$ , and can be classified as trivial ( $\text{Re } \xi = 0$ ) and non-trivial ( $\text{Re } \xi \neq 0$ ). All but one (at  $z = i/2$ ) of the trivial poles are cancelled by the zeros of  $\Gamma(\frac{1}{2} + iz)$ . The non-trivial zeros  $\rho$  of  $\zeta(s)$  lie in the strip  $0 < \text{Re } s < 1$  and the famous Riemann hypothesis implies these zeros are located on the line  $\text{Re } s = \frac{1}{2}$ . For the range of  $w$  values considered in § 4 the hypothesis has been verified by numerical computations, e.g. [8]. We therefore write  $\rho = \frac{1}{2} - it_\rho = \frac{1}{2} - i2w_\rho$  where  $-\infty < t_\rho < +\infty$ ,  $t_\rho \in \mathbb{R}$  and for convenience introduce  $w_\rho = t_\rho/2$ ; both the  $t_\rho$  and the  $w_\rho$  will be referred to as the Riemann zeros here. To express the non-trivial poles in terms of the Riemann zeros, one simply equates  $\rho$  and  $1 - 2i\xi$ , yielding

$$\xi = \xi_\rho = w_\rho - i/4. \quad (3.2)$$

Since  $\text{Im } \xi_\rho = -\frac{1}{4} < 0$  we have, in the terminology of conventional scattering systems, a resonance whenever  $w$  passes through  $w_\rho$ . Investigation of the time delay in § 3.2 and § 4 justifies the association of the poles (3.2) with scattering resonances in this non-conventional system. For later reference we note that the width of the resonances, as determined by  $\text{Im } \xi_\rho$ , is constant whereas the average spacing between adjacent zeros  $w_\rho$  decreases with increasing momentum.

To make the poles  $\xi_\rho = w_\rho - i/4$  explicit in (3.1) we introduce the well known product representation of the  $\zeta$  function [15] in terms of all  $\rho$ :

$$\zeta(s) = \frac{e^{bs}}{2(s-1)\Gamma(1+s/2)} \left( \prod_{\text{Im } \rho < 0} \frac{1}{\rho\rho^*} (\rho - s)(\rho^* - s) \exp[s(\rho^{-1} + \rho^{*-1})] \right) \quad (3.3)$$

where  $b = \ln 2\pi - 1 - \gamma/2$  ( $\gamma$  is the Euler constant) and we have used the fact that if  $\rho$  is a zero then  $\rho^*$  is also a zero. Using (3.3) for  $\zeta(1 + 2iz)$  and  $\zeta(1 - 2iz)$  in (3.1) yields, after straightforward manipulation and the substitutions  $\rho - 1 = -2i\xi_\rho$  and  $\rho^* - 1 = 2i\xi_\rho^*$ ,

$$S(z) = -\pi^{-2iz} e^{i4bz} \frac{(\frac{1}{2} - iz)}{(\frac{1}{2} + iz)} \left( \prod_{w_\rho > 0} \frac{(z + \xi_\rho)(z - \xi_\rho^*)}{(z + \xi_\rho^*)(z - \xi_\rho)} \exp[iz/(w_\rho^2 + \frac{1}{16})] \right). \quad (3.4)$$

For  $\text{Re } z = w > 0$ , each  $\xi_\rho = w_\rho - i/4$  turns out to be a simple pole of  $S(z)$  (provided there are no degenerate zeros of  $\zeta(s)$ , as is consistent with the Riemann hypothesis) and the complex conjugate  $\xi_\rho^* = w_\rho + i/4$  is a zero of  $S(z)$ . For  $\text{Re } z < 0$ ,  $S(z)$  has poles and zeros at  $-\xi_\rho^*$  and  $-\xi_\rho$ , respectively.  $S(z)$  is thus proportional to an infinite product of pole-zero terms. The pole-zero pairs close to the origin, including the trivial pair ( $i/2, -i/2$ ) arising from the  $(\frac{1}{2} - iz)/(\frac{1}{2} + iz)$  factor in (3.4), are depicted in figure 1.

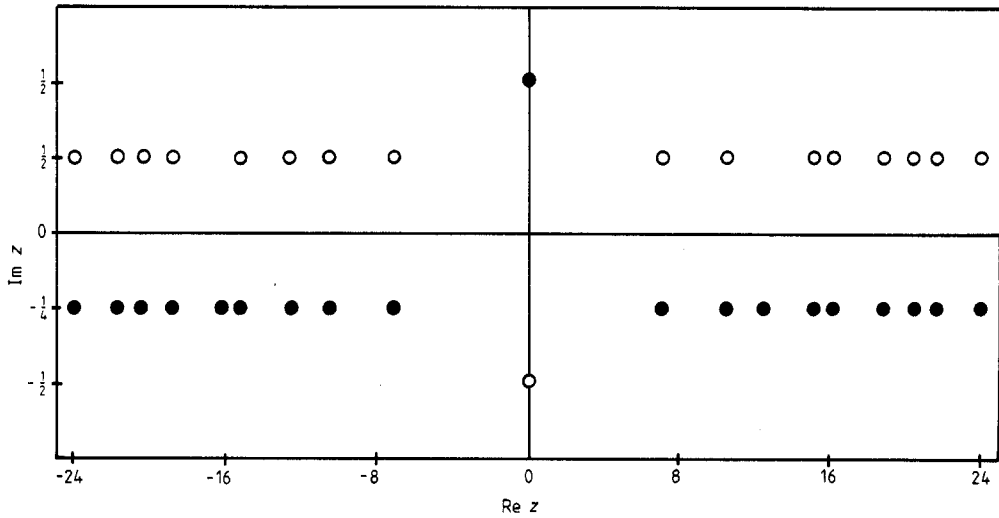


**Figure 1.** Poles (full circles) and zeros (open circles) of the scattering matrix in the vicinity of the origin of the complex momentum plane. All poles and zeros occur as complex conjugate pairs. Scattering resonances are associated with poles having  $\text{Re } z = w \neq 0$ ; the time delay is studied for  $\text{Re } z > 0$ .

### 3.2. Time delay and the Riemann zeros

One route to an expression for the time delay (2.15) in terms of the Riemann zeros is to set  $z = w$  in (3.4) and then use  $T = -iS^*(E) dS(E)/dE$ . It is however less complicated mathematically to begin with

$$\tau_{\text{fl}}(w) = 4 \text{Re} \left( \frac{\zeta'(1+2iw)}{\zeta(1+2iw)} \right) \tag{3.5}$$

and use the logarithmic derivative of the product representation (3.3) of the  $\zeta$  function [15]:

$$\frac{\zeta'(s)}{\zeta(s)} = b - \frac{1}{s-1} - \frac{1}{2} \frac{\Gamma'(1+s/2)}{\Gamma(1+s/2)} + \sum_{\text{Im } \rho < 0} \left( \frac{1}{\rho} + \frac{1}{\rho^*} + \frac{1}{s-\rho} + \frac{1}{s-\rho^*} \right). \tag{3.6}$$

Using (3.6) in (3.5) with  $s = 1 + 2iw$  and  $\rho = \frac{1}{2} - 2iw_{\rho}$  yields

$$\begin{aligned} \tau_{\text{fl}}(w) = 4 \text{Re} \left[ -\frac{1}{2iw} - \frac{1}{2} \frac{\Gamma'(\frac{3}{2} + iw)}{\Gamma(\frac{3}{2} + iw)} \right. \\ \left. + \sum_{w_{\rho} > 0} \left( \frac{\frac{1}{4}}{(\frac{1}{4})^2 + w_{\rho}^2} + \frac{1}{\frac{1}{2} + 2i(w + w_{\rho})} + \frac{1}{\frac{1}{2} + 2i(w - w_{\rho})} \right) \right] \end{aligned} \tag{3.7}$$

or

$$\begin{aligned} \tau(w) = \tau_{\text{bg}}(w) + \tau_{\text{fl}}(w) \\ = 4b - 2 \ln \pi - \frac{1}{\frac{1}{4} + w^2} + \sum_{w_{\rho} > 0} \frac{1}{(\frac{1}{4})^2 + w_{\rho}^2} \\ + \frac{1}{2} \sum_{w_{\rho} > 0} \left( \frac{1}{(\frac{1}{4})^2 + (w + w_{\rho})^2} + \frac{1}{(\frac{1}{4})^2 + (w - w_{\rho})^2} \right) \end{aligned} \tag{3.8}$$



where the definition of  $\tau_{bg}$  [cf (2.15)] has been used to obtain (3.8) from (3.7). A simplified expression for  $\tau$  is obtained by equating  $\tau(w=0) = -4b - 4 + 2 \ln \pi$  (see § 2) to the right-hand side of (3.8) evaluated at  $w=0$ , yielding  $-4b + 2 \ln \pi$  for the fourth term of (3.8); hence,

$$\tau(w) = -\frac{1}{\frac{1}{4} + w^2} + \frac{1}{2} \sum_{w_\rho > 0} \left( \frac{1}{(\frac{1}{4})^2 + (w + w_\rho)^2} + \frac{1}{(\frac{1}{4})^2 + (w - w_\rho)^2} \right). \quad (3.9)$$

At  $w=0$  the second and third terms of (3.9) are equal but, as  $w$  increases from zero, the second term, as well as the first term, decrease relative to the third term. It is therefore expected to be an excellent approximation for sufficiently large  $w > 0$  to write

$$\tau(w) \approx \frac{1}{2} \sum_{w_\rho > 0} \frac{1}{(\frac{1}{4})^2 + (w - w_\rho)^2}. \quad (3.10)$$

The feasibility of using (3.9) to evaluate  $\tau$  numerically (provided, of course, that a sufficient number of Riemann zeros is available) and the validity of (3.10) are assessed in the appendix. In any case the first and second terms of (3.9) each provide a smooth monotonic dependence on  $w$ , whereas the third term provides the interesting fluctuation behaviour (for  $w > 0$ ).

The content of (3.10) is simple. For  $w$  in the neighbourhood of an *isolated* pole  $\xi_\rho$  of  $S$ , the dominant contribution to the time delay is a Lorentzian centred on  $w_\rho$  with half-width  $\Gamma/2 = \frac{1}{4}$ ,

$$\frac{2(\Gamma/2)}{(w - w_\rho)^2 + (\Gamma/2)^2}. \quad (3.11)$$

The time delay approximation (3.11) therefore provides the conventional interpretation of a resonance (at  $w = w_\rho$ ) as a longer-lived scattering event. Equation (3.11) has the same form as the energy dependence of the time delay in the vicinity of an isolated pole of the  $S$  matrix in a simple conventional scattering system [16]. Of course, as the spacing between adjacent  $w_\rho$  becomes less than  $\Gamma$  (i.e. as the resonances begin to overlap), it is anticipated that the signature of *individual* resonances in the time delay should be obliterated; this is addressed in § 4.

#### 4. Numerical results and discussion

In § 4.1 plots of the momentum dependence of the time delay on different  $w$  ranges are compared and discussed. This is followed by a numerical investigation of the autocorrelation function of  $T_{\bar{n}}$  in § 4.2. Details of the numerical calculations which provide the  $\tau$  and  $\tau_{bg}$  values (and hence the  $\tau_{\bar{n}} = \tau - \tau_{bg}$  values) required herein are described in the appendix. It proved computationally expedient to use (3.9) for the evaluation of  $\tau$  since a large number of Riemann zeros were available to us.

##### 4.1. Momentum dependence of $\tau$ and $\tau_{bg}$

Parts (a)–(f) of figure 2 depict  $\tau$  and  $\tau_{bg}$  against  $w$  on six non-adjacent momentum ranges, each spanning 20 momentum units and beginning at  $w = 0, 100, 1000, 5000, 35\,000$  and  $\lambda = 133\,826\,702\,823.5$ , respectively; plotting  $\tau$  instead of  $T = \tau/w$  avoids

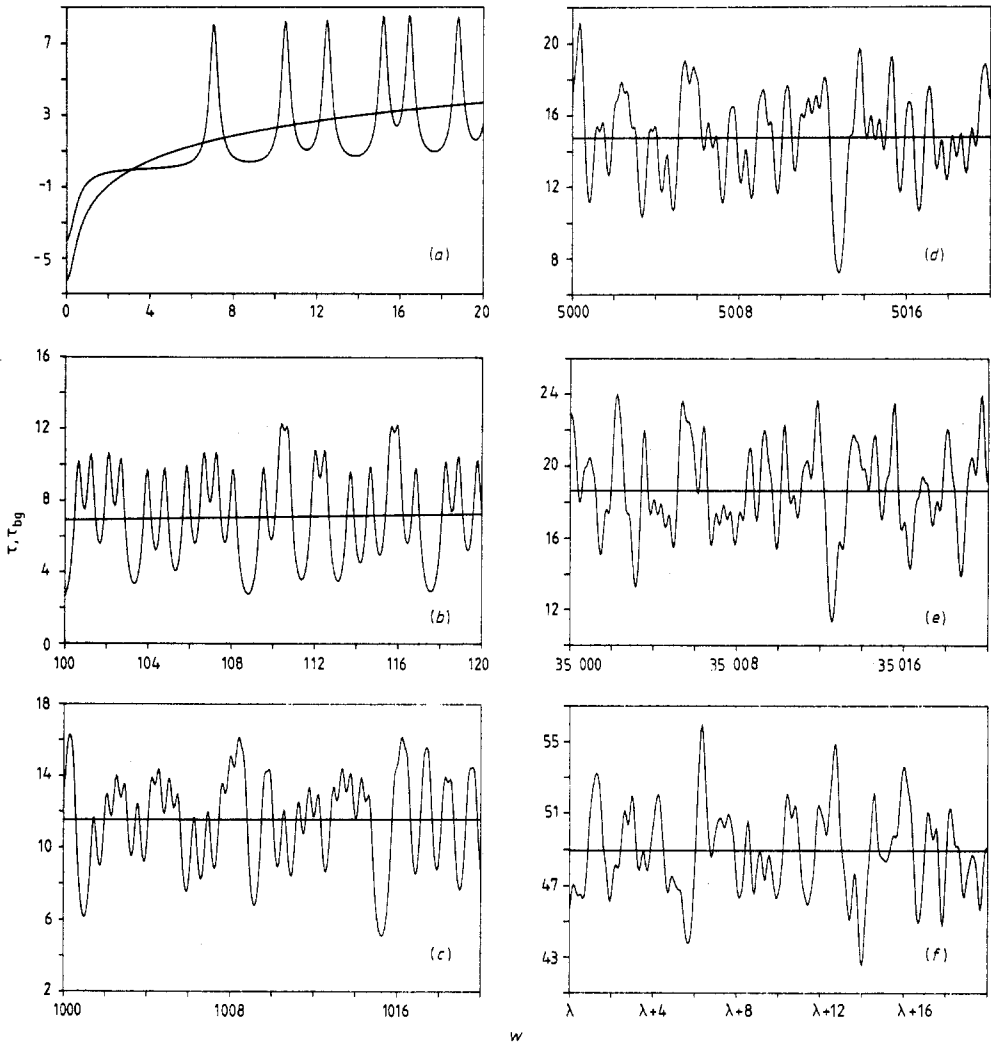


**Figure 2.** Plots of  $\tau$  and  $\tau_{bg}$  on six momentum ranges: (a)  $w = 0-20$ , (b)  $w = 100-120$ , (c)  $w = 1000-1020$ , (d)  $w = 5000-5020$ , (e)  $w = 35\,000-35\,020$ , (f)  $w = \lambda$  to  $\lambda + 20$  with  $\lambda = 133\,826\,702\,823.5$ . The rapidly varying function is  $\tau$  which oscillates about the slowly varying, monotonically increasing function  $\tau_{bg}$ . Not shown is the fluctuating component  $\tau_{fl}$  which is obtained as the difference between  $\tau$  and  $\tau_{bg}$ .

the  $1/w$  scaling arising from the latter. The  $\tau$  values for the first five  $w$  ranges were computed using Odlyzko's set [8] of the first  $\sim 10^5$  zeros whereas those for the  $w$  range of figure 2(f) were computed from his set of about  $10^5$  zeros beginning at the  $10^{12}$  zero. The  $w$  ranges of figures 2(a)-(c) were chosen to correspond to Gutzwiller's plots of  $\delta_{fl}/2$  in figures 5-7 of [3]. The flat curve in each panel is  $\tau_{bg}$  and the oscillating curve is  $\tau$ ; the fluctuating component  $\tau_{fl}$  is simply the difference between the two curves.

Several features of figure 2 are noteworthy. It provides pictorial confirmation for the qualitative momentum dependence attributed to  $\tau_{fl}$  and  $\tau_{bg}$  in § 2.3. That this particular separation of the time delay into fluctuating and background components is indeed the appropriate one was established by demonstrating (numerically) that the

momentum-averaged behaviour of  $T$  is, to an excellent approximation, that of  $T_{bg}^\dagger$ . Introducing the notation  $\langle \dots; w_c \rangle_\Delta = (1/\Delta) \int_{w_c-\Delta/2}^{w_c+\Delta/2} dw \dots$  to indicate an average over a momentum interval  $\Delta$  centred on  $w = w_c$ , we can summarise the numerical results as follows. The approximate relationship  $\langle T; w_c \rangle_\Delta \approx \langle T_{bg}; w_c \rangle_\Delta$  (which implies  $\langle T_{fl}; w_c \rangle_\Delta \approx 0$ ) was found to be valid over a wide range of  $w_c$  and  $\Delta$  values. For example, for a series of intervals of widths  $\Delta = 100, 150, 200$  and  $250$  centred on  $w_c = 200, 1000, 35\,000$  and  $\lambda$  (the last three of which correspond to the lower limits of the  $w$  ranges in figures 2(c), 2(e) and 2(f)) it was found in all cases that  $|\langle T \rangle_\Delta - \langle T_{bg} \rangle_\Delta| / \langle T_{bg} \rangle_\Delta \leq 0.1\%$ .

It is also evident that the character of  $\tau_{fl}$  is changing as  $w$  increases. In figures 2(a) and 2(b) where  $w$  is relatively small, the influence of the scattering resonances is obvious: the peaks in  $\tau$  have the Lorentzian shape predicted by (3.11) and all the maxima of  $\tau$  are positive with respect to  $\tau_{bg}$ . That the resonances are slightly separated on these two  $w$  ranges is readily established by comparing the (constant) resonance width  $\Gamma = 0.5$  with the mean spacing  $D(w)$  of the poles at the midpoint of each  $w$  range in figures 2(a) and 2(b);  $D(w)$  is the reciprocal of the average density  $\rho(w) = \pi^{-1} \ln(w/\pi)$  of the Riemann zeros [11]. In table 1 it is seen that  $\Gamma < D$  and that the maxima in  $\tau$  are in 1:1 correspondence with the zeros on the 0-20 and 100-120  $w$  ranges. For the larger  $w$  values of figures 2(c)-(f), table 1 reveals that there is no longer a 1:1 correspondence between the maxima and the zeros and that, as  $w$  increases, it becomes increasingly unreliable to associate maxima in  $\tau$  with individual poles. In the plots it can be seen that most of the peaks in  $\tau$  do not have a Lorentzian shape and that not all maxima are positive with respect to  $\tau_{bg}$ . In terms of  $\Gamma$  and  $D$ , figures 2(d)-(f) depict  $\tau$  in regions of overlapping resonances ( $\Gamma > D$  in table 1) and figure 2(c) depicts  $\tau$  in what may be called a region of transition from separated to overlapping resonances ( $\Gamma \sim D$  in table 1).

In [3] Gutzwiller estimates the  $w$  value at which the quantal structure in the phase shift should begin to average out, resulting in some sort of 'quasiclassical' behaviour. In terms of the  $S$ -matrix poles, one arrives at his result by equating the mean spacing between poles,  $D(w) = \pi/\ln(w/\pi)$ , to the resonance half-width  $\Gamma/2 = \frac{1}{4}$ , yielding  $w = \pi \exp(4\pi) \approx 9 \times 10^5$ . We simply note that the momentum values of  $w \sim 1.33 \times 10^{11}$  in

Table 1. Selected features of the time delay plots in figure 2.

Panel	$w$ range	Resonance width $\Gamma$	Mean resonance spacing $D$	Number of maxima in $\tau$	Number of poles of $S$
<i>a</i>	0-20	0.5	2.71	7	7
<i>b</i>	100-120	0.5	0.88	23	23
<i>c</i>	1 000-1020	0.5	0.54	30	37
<i>d</i>	5 000-5020	0.5	0.43	33	48
<i>e</i>	35 000-35 020	0.5	0.34	31	60
<i>f</i> †	$\lambda - \lambda + 20$	0.5	0.13	28	155

†  $\lambda = 133\,826\,702\,823.5$ .

† The same numerical results also hold for  $\tau$  over the same ranges of  $w_c$  and  $\Delta$  used in the assessment of properties of  $T$ . In particular, it was found that (a)  $\langle \tau; w_c \rangle_\Delta \approx \langle \tau_{bg}; w_c \rangle_\Delta$  (implying  $\langle \tau_{fl}; w_c \rangle_\Delta = 0$ ), and (b) the normalised autocorrelation function  $c_\tau(\varepsilon; w_c, \Delta)$  of  $\tau$  obtained by substituting  $\tau$  for  $T$  everywhere in (4.2) has essentially the same  $\varepsilon$  dependence as  $c(\varepsilon; w_c, \Delta)$ . The quantity  $\tau = wT$  therefore displays the same 'universal' properties as  $T$ . It appears that an analytical derivation of these properties in terms of properties of the Riemann zeros might be possible via mathematical analysis of (3.9).

figure 2(*f*) lie far beyond this estimate for the transition from quantum to classical-like behaviour. However figures 2(*d*)-2(*f*), all of which lie in the  $\Gamma > D$  region, are qualitatively similar and provide no evidence for such a distinction in regard to the time delay. A quantitative characterisation of  $T$  on widely separated momentum ranges is described in § 4.2.

#### 4.2. A characterisation of $T_{\bar{n}}$

Theoretical results for the description of the time delay appear to be confined to its relationship to other scattering quantities or system properties [16, 17, 18] and do not describe its distributive or statistical properties. We therefore confine ourselves to numerical computations and examine the autocorrelation function of  $T_{\bar{n}}$ , motivated by Ericson and Mayer-Kuckuk's [19] study of this property for differential cross sections in the strongly overlapping resonance region.

The autocorrelation function  $C$  is defined in the usual manner:

$$\begin{aligned} C(\varepsilon; w_c, \Delta) &= \langle [T(w) - T_{bg}(w)][T(w + \varepsilon) - T_{bg}(w + \varepsilon)] \rangle_{\Delta} \\ &= \langle T_{\bar{n}}(w) T_{\bar{n}}(w + \varepsilon) \rangle_{\Delta} \end{aligned} \quad (4.1)$$

where  $\langle \dots \rangle_{\Delta}$  indicates averaging over a momentum range  $\Delta$  centred on  $w_c$ . To facilitate comparison on different  $w$  ranges we introduce the related reduced or 'normalised' quantity

$$c(\varepsilon; w_c, \Delta) = \langle T_{\bar{n}}(w) T_{\bar{n}}(w + \Delta) \rangle_{\Delta} / \langle T_{\bar{n}}^2(w) \rangle_{\Delta} \quad (4.2)$$

which has the value one at  $\varepsilon = 0$ . Figures 3(*a*) and 3(*b*) show plots of  $c(\varepsilon; w_c, \Delta)$  for  $w_c = 200$  and  $w_c = \lambda = 133\,826\,702\,823.5$ , respectively; in each case  $\Delta = 200$  and  $\varepsilon$  ranges from 0 to 10. The averages in (4.2) were evaluated by numerical quadrature (both Simpson's rule and the trapezoidal rule) and their convergence established by decreasing the integration step size until successive  $c(\varepsilon; w_c, \Delta)$  values agreed within 0.001. The following features of figure 3 merit some discussion.

(i) Although the mean spacing between poles of  $S$  varies by a factor of  $\sim 6$  between figures 3(*a*) and 3(*b*) ( $D(w) = 0.76$  at  $w = 200$  whereas  $D(w) = 0.13$  at  $w = \lambda$ ), the  $c(\varepsilon; w_c, \Delta)$  plots in figure 3 and corresponding plots (not shown) with  $w_c = 500, 1000, 5000$  and  $35\,000$  are almost indistinguishable from each other on the scale of the plots. The expected fluctuations in  $c(\varepsilon; w_c, \Delta)$  due to a finite averaging interval were observed as  $\Delta$  was varied from 100 to 300 in increments of 50 but were barely discernible on the scale used in figure 3. This shows that the autocorrelation function of  $T_{\bar{n}}$  is approximately independent of  $w_c$  and  $\Delta$ , i.e.

$$c(\varepsilon; w_c, \Delta) \approx c(\varepsilon) \quad (4.3)$$

and that it therefore provides a characterisation of the fluctuations in the time delay of our model system which is 'universal' in the sense that it applies regardless of the range of  $w$ , in particular whether  $\Gamma > D(w)$ ,  $\Gamma < D(w)$ , or  $\Gamma \sim D(w)$ . The detailed shape of  $c(\varepsilon)$  can undoubtedly be traced back to the poles of  $S$  via the expression (3.9) for  $\tau$  but a more interesting question is whether the shape is a particular property of the model system or is a generic property arising from the GUE statistics of the real parts of the poles, i.e. the imaginary parts of the Riemann zeros.

(ii) Examination of either plot in figure 3 reveals that  $c(\varepsilon)$  decays from 1 at  $\varepsilon = 0$  to  $\sim 0$  at  $\varepsilon \sim 0.4$ . For  $0.4 < \varepsilon < 10$ ,  $c(\varepsilon)$  oscillates about zero but shows no sign of approaching zero with increasing  $\varepsilon$ , implying the existence of long-range (i.e.  $\varepsilon \gg \Gamma$ ,

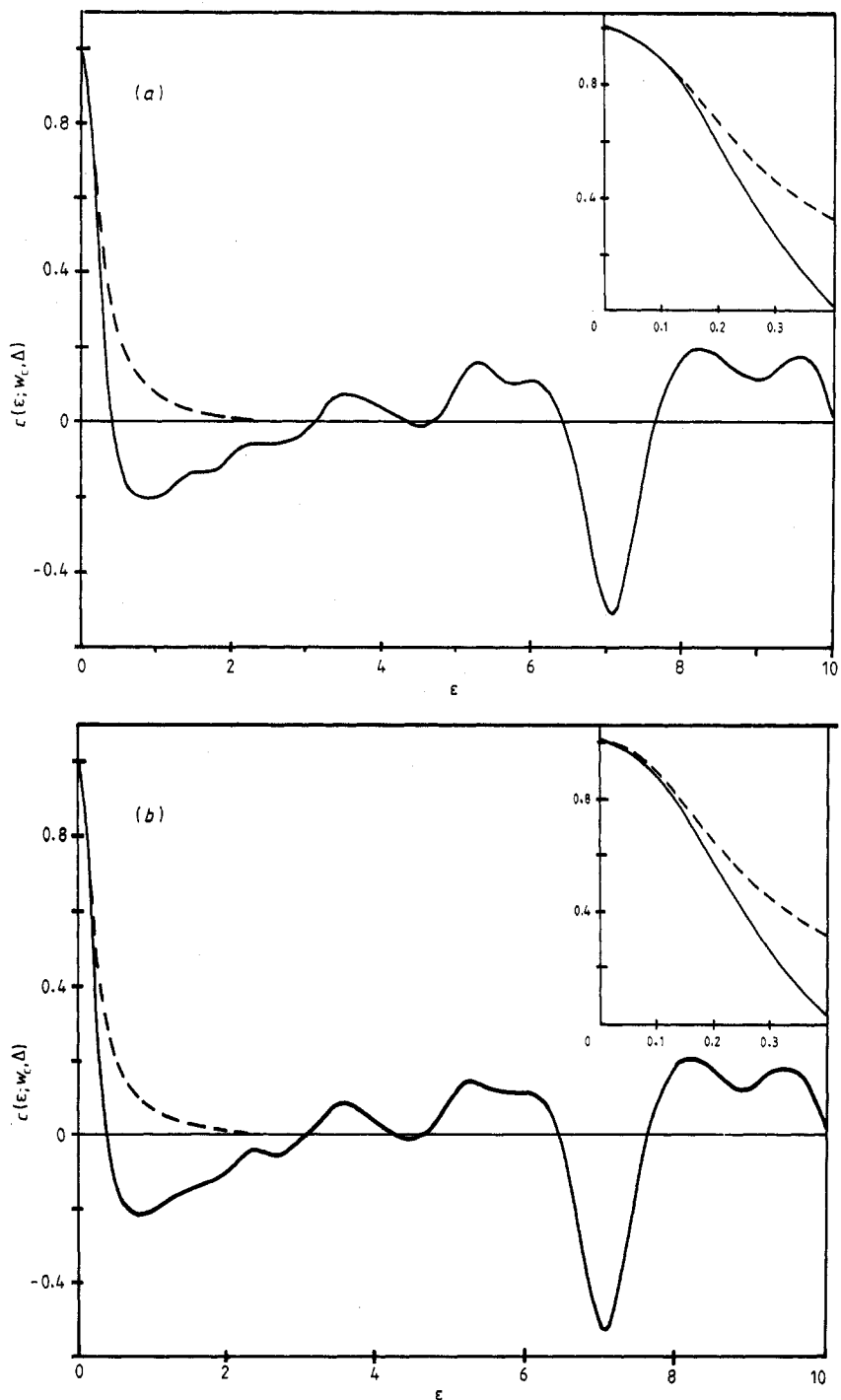


**Figure 3.** Plots of the normalised time delay autocorrelation function  $c(\varepsilon; w_c, \Delta)$  as obtained by averaging over a momentum interval  $\Delta$  centred on (a)  $w_c = 200$ , and (b)  $w_c = \lambda = 133\,826\,702\,823.5$ . The broken curve is a Lorentzian whose half-width  $\beta$  is determined numerically from the small- $\varepsilon$  behaviour of  $c$ ;  $\beta = 0.28$  and  $0.27$  in panels (a) and (b), respectively.

$D(w)$  correlations in  $T_n$ . Ignoring the prominent negative correlation at  $\varepsilon \sim 7$  in figure 3, one is struck by a remarkable qualitative similarity between figure 3 and experimentally determined cross section energy autocorrelation functions depicted in [20]. The oscillations in the latter at large  $\varepsilon$  values have been attributed to averaging over a finite energy interval. On the other hand, the dominant oscillations in  $c(\varepsilon)$  were found to be independent of the averaging interval, as described in (i). The effect of a finite range of data on cross section fluctuation analysis has been addressed by Dallimore and Hall [21] but an analogous treatment for time delay is not available.

(iii) In an attempt to provide a quantitative understanding of the small- $\varepsilon$  behaviour of  $c(\varepsilon)$ , we assessed the suitability of a Lorentzian autocorrelation function  $\tilde{c}(\varepsilon)$  with half-width  $\beta$ :

$$\tilde{c}(\varepsilon) = \frac{\beta^2}{\varepsilon^2 + \beta^2}. \quad (4.4)$$

This arbitrary choice is motivated by the theoretical work of Ericson and Mayer-Kuckuk [19] who obtain (4.4) as the cross section energy autocorrelation function for a model in which the scattering amplitude is a sum of resonance terms of constant width  $2\beta \gg d$ , where  $d$  is the mean resonance energy level spacing. Their prediction has been verified, for small  $\varepsilon$ , by comparison with experimentally determined cross section autocorrelation functions in [20]. The broken curves in figures 3(a) and 3(b) are  $\tilde{c}(\varepsilon)$  with  $\beta = 0.28$  and 0.27, respectively; the excellent agreement between  $\tilde{c}(\varepsilon)$  and  $c(\varepsilon; w_c, \Delta)$  at small  $\varepsilon$  is evident in the insets of figure 3. For all other values of  $w_c$  considered the same level of agreement was obtained and the  $\beta$  values were between 0.27 and 0.28.

The  $\beta$  values were determined by expanding each function about  $\varepsilon = 0$  to second order in  $\varepsilon$  and comparing coefficients, namely

$$c(\varepsilon; w_c, \Delta) \approx (1 + \varepsilon \langle T_n(w) T_n'(w) \rangle_\Delta + \frac{1}{2} \varepsilon^2 \langle T_n(w) T_n''(w) \rangle_\Delta) / \langle T_n^2(w) \rangle_\Delta \quad (4.5)$$

$$\tilde{c}(\varepsilon) \approx 1 - \varepsilon^2 / \beta^2.$$

For all values of  $w_c$  and  $\Delta$ ,  $\langle T_n(w) T_n'(w) \rangle_\Delta \approx 0$ , as required of the Lorentzian form, and the half-width  $\beta$  was then determined numerically from

$$\beta^2 = - \frac{2 \langle T_n(w) \rangle_\Delta}{\langle T_n(w) T_n''(w) \rangle_\Delta}. \quad (4.6)$$

The interesting feature of the analysis is the information contained in the  $\beta$  values: they are essentially constant over a wide range of  $w_c$  values, supporting the suggestion in (i) that  $c(\varepsilon)$  provides a universal characterisation of  $T_n$ . The  $\beta$  values are approximately equal to  $\Gamma/2$  where  $\Gamma = 0.5$  is the constant width of the resonances in our model. Thus it appears that in the  $\Gamma > D$  region the width of *individual* resonances can be recovered from the time delay autocorrelation function whereas this information is obscured in time delay against  $w$  plots. Whether the relationship  $\beta \approx \Gamma/2$  is particular to the model or is of more general applicability is a question requiring further study.

### Acknowledgments

It is a pleasure to acknowledge the support of this research by the Natural Sciences and Engineering Research Council of Canada and by the Advisory Research Council

of Queen's University. DMW is grateful to Professor Paul Brumer for bringing the existence of this model system to his attention. The authors thank Professor M V Berry for suggesting the poles-of-the- $S$ -matrix approach to our treatment and Dr A D Odlyzko for providing the sets of Riemann zeros used in this work.

## Appendix

The quantity  $\tau$  is computed from (3.9) by changing the infinite summations to finite ones as follows:

$$\tau(w) \approx \tau(w; N) \equiv -\frac{1}{\frac{1}{4} + w^2} + \frac{1}{2} \sum_{i=1}^{2N} \frac{1}{(\frac{1}{4})^2 + (w + w_i)^2} + \frac{1}{2} \sum_{i=\max(k-N, 1)}^{k+N} \frac{1}{(\frac{1}{4})^2 + (w - w_i)^2}. \quad (\text{A1})$$

Here  $N$  is an integer chosen large enough to ensure that (A1) converges within a specified tolerance (discussed below); the poles  $w_p$  have been relabelled  $w_i$ ;  $k$  is such that  $w_k$  is the pole closest to  $w$ ; the lower summation limit  $\max(k - N, 1)$  in the third term ensures that  $i \geq 1$  for  $k - N \leq 0$  (i.e. for sufficiently large  $N$  or sufficiently small  $w$ ). The zeros  $t_i/2 = w_i$  used in our evaluation of  $\tau$  via (A1) are those computed by Odlyzko [8] and the relative ease of computation of  $\tau$  afforded by (A1) relies on the considerable numerical effort invested in the computation of the zeros. An alternative route to  $\tau$  is provided by (2.15) which explicitly involves the  $\zeta$  function and its first derivative. The increasing numerical difficulty, with increasing  $w$ , of evaluating series representations of the  $\zeta$  function have been noted by Gutzwiller [3]. However, to assess the accuracy of (A1) we evaluated, for  $w \leq 5000$ ,

$$\tau(w) = -2 \ln \pi + 2 \operatorname{Re} \left( \frac{\Gamma'(\frac{1}{2} + iw)}{\Gamma(\frac{1}{2} + iw)} \right) + 4 \operatorname{Re} \left( \frac{\zeta'(1 + 2iw)}{\zeta(1 + 2iw)} \right) \quad (\text{A2})$$

using the Euler-Maclaurin summation formulae [22] for  $\zeta$  and  $\zeta'$ , yielding an 'exact'  $\tau(w) \equiv \lim_{N \rightarrow \infty} \tau(w; N)$ .

Our approach to ensuring that (A1) provide a reliable estimate of  $\tau$  is as follows. For selected  $w$  values in the ranges 0-20, 100-120, 1000-1020, and 5000-5020 of figures 2(a)-(d), (A2) was evaluated and compared with the  $\tau(w; N)$  values obtained from (A1) with successively larger  $N$  values. For the 0-20 and 100-120 ranges,  $N$  values of 700 and 800, respectively, are found to provide approximate  $\tau$  values which are less than the exact values by at most  $\sim 0.003$ . Because the lower limit in the second summation of (A1) is unity for these  $N$  and  $w$  values, the number of terms contributing to the second summation of (A1) is  $\sim 700$  and  $\sim 890$  (instead of  $2N + 1$ ) for the 0-20 and 100-120  $w$  ranges; the exact number of contributing terms depends weakly on  $w$ . For the 1000-1020 and 5000-5020  $w$  ranges, approximate  $\tau$  values differing from exact values by at most  $\sim 0.003$  were achieved with  $N = 1000$  and 2000, respectively; the number of terms contributing to the second summation of (A1) is now  $2N + 1$  since  $k > N$  in each case. For  $w$  ranges beyond  $w = 5020$  no attempt was made to obtain exact  $\tau$  values and  $N$  was determined solely by a convergence criterion suggested by  $\tau(w; N)$  results in the 1000-1020 and 5000-5020 ranges; namely, that increasing  $N$  by 50% for these ranges increased  $\tau(w; N)$  by  $\sim 0.001$  or less if  $\tau(w; N)$  was within  $\sim 0.003$  of  $\tau(w)$ . Applying this criterion to the 35 000-35 020 and  $\lambda$  to  $\lambda + 20$   $w$  ranges yields  $N$  values of 4000 and 20 000, respectively. The increase in  $N$  with  $w$  is to be expected on the basis of the well known  $\ln w$  increase in the mean density of the Riemann zeros.

It is reassuring to verify numerically the approximation (3.10) of neglecting the first and second terms of (A1). For example,  $\tau(w = 100; N = 800) = 2.678$  with the first and second terms of (A1) contributing  $-1.0 \times 10^{-4}$  and  $4.4 \times 10^{-3}$ , respectively, for a combined contribution to  $\tau$  of 0.16% whereas  $\tau(w = 1000; N = 1000) = 13.000$  with first and second terms of  $-1.0 \times 10^{-5}$  and  $4.0 \times 10^{-4}$  for a combined contribution to  $\tau$  of 0.003%. The approximation is seen to improve with increasing  $w$  as expected.

## References

- [1] Series C 1987 *Proc. R. Soc. A* **413** 171
- [2] Balazs N L and Voros A 1986 *Phys. Rep.* **143** 109  
Balazs N L, Schmit C and Voros A 1987 *J. Stat. Phys.* **46** 1067
- [3] Gutzwiller M 1983 *Physica D* **7** 341
- [4] Jaworski W and Wardlaw D M *Preprint*
- [5] Lax P D and Phillips R S 1976 *Scattering Theory for Automorphic Functions* (Princeton, NJ: Princeton University Press)
- [6] Kubota T 1973 *Elementary Theory of Eisenstein Series* (Tokyo: Kodansha Limited)
- [7] Weidenmüller H A 1986 *Comment. Nucl. Part. Phys.* **16** 199
- [8] Odlyzko A M 1987 *Math. Comput.* **48** 273
- [9] Montgomery H L 1973 *Proc. Symp. Pure Math.* **24** 181; 1975 *Proc. Int. Congr. Math., Vancouver 1974* ed R D James pp 511–8
- [10] Odlyzko A M *unpublished*
- [11] Berry M V 1986 *Quantum Chaos and Statistical Nuclear Physics* (Lecture Notes in Physics **263**) ed T H Seligman and H Nishioka (New York: Springer) pp 1–17; 1987 *Proc. R. Soc. A* **413** 183
- [12] Taylor J R 1972 *Scattering Theory* (New York: Academic)
- [13] Jaworski W and Wardlaw D M 1988 *Phys. Rev. A* **37** 2843
- [14] Lebedev N N 1972 *Special Functions and Their Applications* (New York: Dover)
- [15] Titchmarsh E C 1951 *Theory of the Riemann Zeta Function* (Oxford: Clarendon)
- [16] Smith F T 1960 *Phys. Rev.* **118** 349  
Celenza I and Tobocman W 1968 *Phys. Rev.* **174** 1115
- [17] Osborn T A and Tsang T Y 1976 *Ann. Phys.* **101** 119  
Wardlaw D M, Brumer P and Osborn T A 1982 *J. Chem. Phys.* **76** 4916  
Bollé D and Osborn T A 1979 *J. Math. Phys.* **20** 1121
- [18] Bauer M, Mello P A and McVoy K W 1979 *Z. Phys. A* **293** 151
- [19] Ericson T and Mayer-Kuckuk T 1966 *Ann. Rev. Nucl. Sci.* **16** 183
- [20] Van Brentano P, Ernst J, Häusser O, Mayer-Kuckuk T, Richter A and Von Witsch W 1964 *Phys. Lett.* **9** 48
- [21] Dallimore P J and Hall I 1965 *Phys. Lett.* **18** 138
- [22] Edwards H M 1974 *Riemann's Zeta Function* (New York: Academic)